

# Photocatalytic reduction of CO<sub>2</sub> over TiO<sub>2</sub> nanowires catalyst

Andrey Tarasov<sup>1\*</sup>, Sergey Dubkov<sup>1</sup>, Vigdrovich Evgeny<sup>1</sup>, Fedyanina Maria<sup>1</sup>, Ryazanov Roman<sup>2</sup>, Sirotina Anna<sup>3</sup> and Dmitriy Gromov<sup>1</sup>

<sup>1</sup>National Research University “MIET”, 124498 Moscow, Zelenograd, Russia

<sup>2</sup>SMC “Technological centre”, 124498 Moscow, Zelenograd, Russia

<sup>3</sup>Institute of Nanotechnology of Microelectronics of the Russian Academy of Sciences, 115487 Moscow, Russia

**Abstract.** TiO<sub>2</sub> is one of the most common photocatalysts at the moment. One-dimensional TiO<sub>2</sub>, which has a high specific surface area, is of particular interest. The properties of such nanowires will largely depend on the phase composition, which affects the width of the optical band gap. This paper presents the results of a study of the photocatalytic activity of TiO<sub>2</sub> nanowires depending on the phase composition using the reduction of CO<sub>2</sub> to methane and methanol as an example. The formation of TiO<sub>2</sub> nanowires was carried out using a hydrothermal synthesis method from a commercial TiO<sub>2</sub> powder. After synthesis, the nanowires were thermally treated in air to obtain nanowires with different phase compositions. The morphology and phase composition of TiO<sub>2</sub> nanowires were studied. The resulting nanowires had a size of about 8 μm and a diameter of about 330 nm.

## 1 Introduce

One of the solutions to environmental and energy problems could be the photocatalytic conversion of CO<sub>2</sub> into useful organic compounds. The process itself is similar to photosynthesis, which occurs in plants. As a result of a photocatalytic reaction, CO<sub>2</sub> can be reduced to various chemical compounds such as methane (CH<sub>4</sub>), methanol (CH<sub>3</sub>OH), formic acid (HCOOH), carbon monoxide (CO) and others [1]. Among these compounds, methane is of the greatest interest. It is a precursor to many organic compounds (acetic acid, formaldehyde, etc.) [2] and a fuel in fuel cells [3]. Fuel cells can be used in autonomous devices, hybrid vehicles and aircraft. During the photocatalytic reaction of CO<sub>2</sub> reduction to methane, many compounds are formed, among which methanol is one of the most important [4].

Photocatalytic reduction of CO<sub>2</sub> can take place on a variety of materials: as on semiconductors [5-7], and on metals [8]. One of the promising is semiconductor TiO<sub>2</sub>, which has high photostability, high catalytic activity in the UV range, low cost and minimal environmental impact. TiO<sub>2</sub> can exist in four different crystalline phases: anatase

---

\* Corresponding author: [bogger4@gmail.com](mailto:bogger4@gmail.com)

(tetragonal), rutile (tetragonal), brookite (orthorhombic), and TiO<sub>2</sub>(B) (monoclinic). The transition between phases is carried out during heat treatment. The greatest effect of increasing the specific surface area is observed on one-dimensional nanoobjects. Nanowires have a high aspect ratio, which has a positive effect on the absorption of incident radiation. The high crystallinity of nanowires reduces the probability of recombination of charge carriers and the geometry of nanowires promotes diffusionless transfer of charge carriers along the longest direction of the nanowire. The paper [9] presents the results of photocatalytic decomposition of an organic dye by TiO<sub>2</sub> nanowires annealed at different temperatures in vacuum. Depending on the annealing temperature, the crystalline phase of the samples changed which affects the photocatalytic activity. However, the photocatalytic reduction of CO<sub>2</sub> to methane has not been investigated.

This paper demonstrates the preparation of TiO<sub>2</sub> nanowires by the hydrothermal synthesis method, the effect of annealing temperature on the crystalline phase and optical properties of TiO<sub>2</sub>, and also presents the results of a study of the photocatalytic activity of CO<sub>2</sub> reduction to methane and methanol using nanowires with different phase compositions.

## 2 Experimental

### 2.1 Synthesis of TiO<sub>2</sub> nanowires

TiO<sub>2</sub> nanowires were obtained by hydrothermal synthesis. For synthesis 0.6 g of commercial TiO<sub>2</sub> powder "Degussa P25" was added to 50 ml of 10 M sodium alkali (NaOH) aqueous solution and stirred on a magnetic stirrer (HJ-3) for 30 minutes. Then the resulting suspension was transferred into a fluoroplastic container of the autoclave. The filling factor was 0.5. The autoclave was heated in a muffle furnace (Project 30/1250) to 250°C and kept for 12 hours. After the end of the synthesis time, the autoclave was cooled to room temperature. The resulting nanowires were washed in a 12 M aqueous HCl solution for 2 hours with constant stirring. Removal of HCl residues was carried out by repeated washing of nanowires in deionized water at a temperature of 80°C with constant stirring. Then the nanofibers were separated by vacuum filtration. Washing was carried out to normal pH. The washed nanowires were dried in an oven. To obtain crystalline TiO<sub>2</sub>, the nanowires were additionally annealed in air for 4 hours at temperatures of 500, 700, and 900°C.

### 2.2 Physicochemical characterization

Diffuse reflectance spectra of powder samples were measured on a Cary 5000 UV-VIS-NIR spectrophotometer with an integrating sphere (Agilent, USA) in the wavelength range from 200 to 800 nm. Reflection spectra were recorded with a spectral resolution of 1 nm.

The phase composition of the photocatalysts was studied on a PANalytical X'Pert Pro MPD diffractometer (Malvern Panalytical Ltd., Malvern, United Kingdom) with a CuK $\alpha$  radiation source ( $\lambda = 1.5418 \text{ \AA}$ ) in the range  $2\theta$  5–90°. The mass fraction of TiO<sub>2</sub> polymorphs was estimated using the reference intensity ratio (RIR) method. The surface morphology of the studied samples was studied using a HITACHI scanning electron microscope (Hitachi High-Tech, Tokyo, Japan) equipped with an EDS energy dispersive spectrometer (Thermo Noran, Worona Road Madison, WI, USA).

### 2.3 Photocatalytic activity measurements

The photocatalytic activity of the samples was measured in a thermostatically controlled flow reactor equipped with a quartz window (Figure 1). The mass of the sample for each

photocatalytic reaction was about 0.2 g. The sample was irradiated with high-pressure mercury lamps POLAMP LRF 400W. The surface area of the photocatalyst subjected to UV irradiation was 10.18 cm<sup>2</sup>. The process conditions were as follows: reactor temperature, 30 °C; reaction mixture, 5% vol. H<sub>2</sub>O/95% vol. CO<sub>2</sub>; and the total gas flow is 0.8 ml/min. The first measurements were carried out after at least 2 hours in the flow. The reaction products were analyzed on an on-line gas chromatograph equipped with a flame ionization detector and an HP PLOT/Q capillary column. The calculation of the yield of reaction products was carried out using the expression:

$$Y_{\text{compound}} \left( \frac{\mu\text{mol}}{\text{g} \cdot \text{h}} \right) = \frac{\text{Molar flow rate}_{\text{compound}}}{g_{\text{catalyst}} \times 60} \quad (1)$$

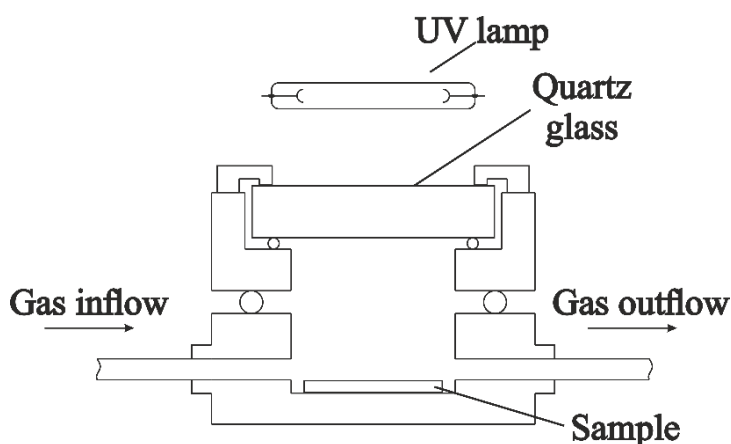


**Fig. 1.** Schematic representation of a temperature-controlled flow reactor

### 3 Results and discussion

Figure 2 shows the SEM image and the histogram of the nanowire length distribution. The observed nanowires have an average length of about 8 μm and an average diameter of about 330 nm. It should be noted that the distribution along the length of the nanowires has a normal form (Fig. 2b).

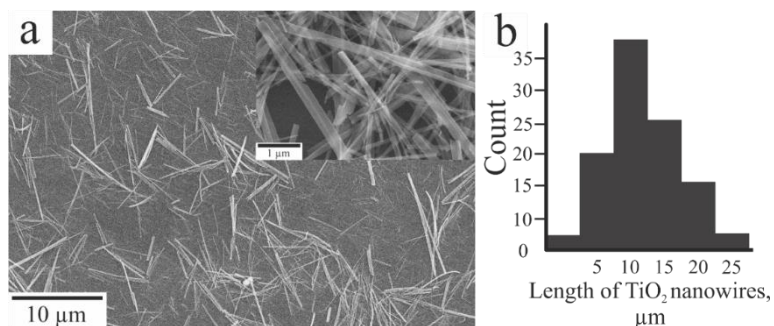


**Fig. 2.** SEM images of TiO<sub>2</sub> nanowires (a) and nanowire length distribution histogram (b)

Figure 3 shows X-ray patterns of TiO<sub>2</sub> nanowires annealed at different temperatures in an air atmosphere. For the sample of nanowires that did not undergo annealing, diffuse low-intensity peaks are observed, which indicates a low degree of crystallinity. The observed low

intensity peaks can be identified as a mixture of hydrogen titanate and sodium titanate. As can be seen in Figure 3, a mixture of TiO<sub>2</sub>(B) and anatase crystalline phases is identified in the sample annealed at 500°C. With an increase in the annealing temperature, TiO<sub>2</sub>(B) completely transforms into anatase and the formation of rutile begins, which can be seen in the diffraction pattern of the sample after annealing at a temperature of 700°C. The rutile/anatase phase ratio is about 30/70% [10]. At 900°C, rutile becomes the dominant phase, but it can be noted that the presence of anatase is retained. The rutile/anatase phase ratio for this annealing is about 75/25%.

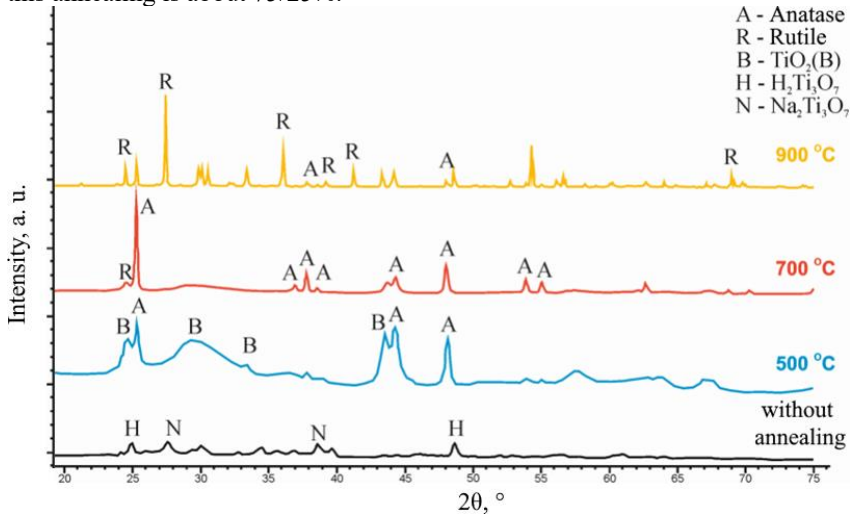


**Fig. 3.** X-ray diffraction patterns of synthesized TiO<sub>2</sub> nanowires samples

The optical properties of samples of the initial and annealed nanowires were studied by measuring the spectral dependences of diffuse reflectance in the UV and visible regions of the spectrum. From the diffuse reflection data, the spectral dependences of the absorption of the samples were obtained using the Kubelka-Munk function [11]:

$$[F(R_d)] = \left[ \frac{(1 - R_d)^2}{2R_d} \right] \tag{2}$$

where  $R_d$  is the diffuse reflectance and  $F(R_d)$  is a value proportional to the absorption coefficient. The optical band gap of all samples was estimated by determining the intersection point of the tangent drawn to the linear section of the energy dependence  $F(R_d)$  with the abscissa axis, as shown in Figure 4.

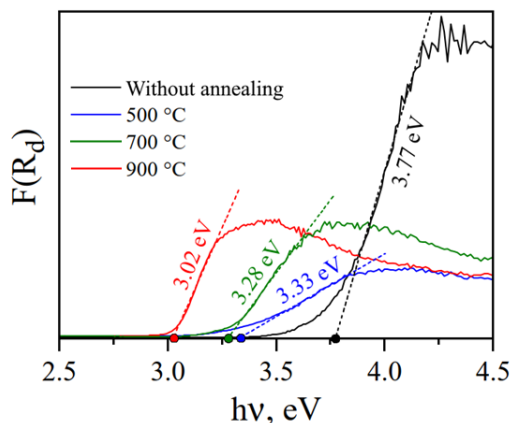


**Fig. 4.** Tautz plot of diffuse reflectance of TiO<sub>2</sub> nanowires

Nanowires that have not undergone annealing have the largest band gap, which may indicate a low degree of crystallinity of the samples. With increasing temperature, a decrease in the optical band gap in TiO<sub>2</sub> samples is observed. This fact can be explained by the appearance of new crystalline phases, such as TiO<sub>2</sub>(B), anatase, and rutile, as well as their mixtures. The optical band gap of a sample annealed at 500°C is about 3.33 eV. This sample is a mixture of crystalline phases of TiO<sub>2</sub>(B) and anatase, having a band gap of about 3.2 [12] and 2.8 – 2.9 eV [13] respectively. Nanowires annealed at 700°C also have an optical band gap close to that of anatase. The sample annealed at 900°C showed an optical band gap of 3.02 eV, which is close to pure rutile with a band gap of about 3.00 eV [14].

The results of photocatalytic measurements showed that the activity of TiO<sub>2</sub> nanowires varied significantly depending on their annealing temperature and the duration of photocatalytic reactions (Figure 5). In general, all samples showed high activity at the beginning of the process, i.e., 1–2 hours after the start of irradiation of the photocatalyst surface. Further, the photocatalytic activity gradually decreased over time. This may be due to a decrease in the surface area of the nanowires due to the reversible adsorption of hydroxyl groups on the surface of the nanowires [15]. The main photocatalytic products were methane and methanol (Figure 5). Carbon monoxide or other organic products were not observed. It is worth noting the low yield of methanol compared to methane. This indicates the selectivity of reactions occurring on the surface of nanowires. The yield of methanol differs slightly for samples annealed at different temperatures. The smallest yield was shown by the sample annealed at 500°C. Samples after heat treatment at 700 and 900°C demonstrate approximately the same yield of methanol. The opposite picture is observed in the study of the release of methane from the samples. With an increase in the heat treatment temperature of nanowires, the yield of methane decreases. The highest yield of methane was found for a sample annealed at 500°C, consisting of a mixture of crystalline phases of TiO<sub>2</sub>(B) and anatase. The production of methane in this sample is higher than in samples annealed at 700 and 900°C by 20 and 22%, respectively.

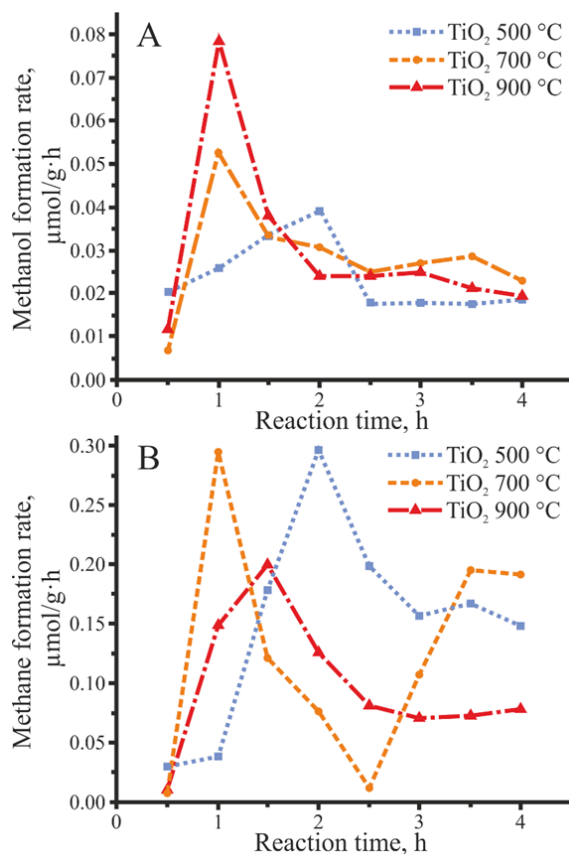


**Fig. 5.** Photocatalytic activity of TiO<sub>2</sub> nanowires: formation rate of methanol (a) and methane (b)

## 4 Conclusions

The TiO<sub>2</sub> nanowires obtained by hydrothermal synthesis had an average length of about 8 μm and a diameter of about 330 nm. The study of the phase composition by XRD after annealing in air for 4 hours showed the appearance of phases TiO<sub>2</sub>(B)/anatase, anatase/rutile (70/30%) and anatase/rutile (25/75%) at temperatures of 500, 700 and 900 °C, respectively. The appearance of new phases is accompanied by a change in the optical band gap. As the annealing temperature increased, the optical band gap decreased. The study of CO<sub>2</sub> reduction on TiO<sub>2</sub> nanowires demonstrated the presence of two main reaction products: methanol and methane. However, the yield of methanol is negligible compared to the yield of methane. TiO<sub>2</sub> annealed at 500°C showed a methane yield 20 (annealed 700 °C) and 22% (annealed 900 °C) higher. The presence of selective reduction of CO<sub>2</sub> to methane is a promising direction for the use of TiO<sub>2</sub> nanowires as a photocatalyst for the production of methane.

This research was funded by the Russian Science Foundation (Project No. 22-19-00654)

## References

1. J. Hong, W. Zhang, J. Ren, and R. Xu, *Anal. Methods* **5**, 1086 (2013)
2. L. Chen, Z. Qi, S. Zhang, J. Su, and G. A. Somorjai, *Catalysts* **10**, 858 (2020)

3. R. Kumar, A. Kumar, and A. Pal, *International Journal of Hydrogen Energy* **47**, 34831 (2022)
4. E. Karamian and S. Sharifnia, *Journal of CO<sub>2</sub> Utilization* **16**, 194 (2016)
5. F. Fang, Y. Liu, X. Sun, C. Fu, Y. Prakash Bhoi, W. Xiong, and W. Huang, *Applied Surface Science* **564**, 150407 (2021)
6. B. Khan, F. Raziq, M. Bilal Faheem, M. Umar Farooq, S. Hussain, F. Ali, A. Ullah, A. Mavlonov, Y. Zhao, Z. Liu, H. Tian, H. Shen, X. Zu, S. Li, H. Xiao, X. Xiang, and L. Qiao, *Journal of Hazardous Materials* **381**, 120972 (2020)
7. X. Ma, D. Li, Y. Jiang, H. Jin, L. Bai, J. Qi, F. You, and F. Yuan, *Journal of Colloid and Interface Science* **628**, 768 (2022)
8. J. You, M. Xiao, Z. Wang, and L. Wang, *Journal of CO<sub>2</sub> Utilization* **55**, 101817 (2022)
9. P. Makal and D. Das, *Applied Surface Science* **455**, 1106 (2018)
10. K. Y. Jung and S. B. Park, *Journal of Photochemistry and Photobiology A: Chemistry* **127**, 117 (1999)
11. E. L. Simmons, *Appl. Opt.* **14**, 1380 (1975)
12. R. López and R. Gómez, *J Sol-Gel Sci Technol* **61**, 1 (2012)
13. P. Makal and D. Das, *Journal of Environmental Chemical Engineering* **7**, 103358 (2019)
14. D. A. H. Hanaor and C. C. Sorrell, *J Mater Sci* **46**, 855 (2011)
15. Y. Y. Maruo, T. Yamada, and M. Tsuda, *J. Phys.: Conf. Ser.* **379**, 012036 (2012)